JOURNAL OF THERMOPHYSICS AND HEAT TRANSFER
Vol. 25, No. 2, April–June 2011

Heat Flux Calibration Measurement Using the Noninteger System Identification Method for Cooled Surfaces

Stefan Löhle* and Ulf Fuchs†
Universität Stuttgart, D-70569 Stuttgart, Germany

DOI: 10.2514/1.T3631

A method is presented that allows the determination of the net heat flux to surfaces from in-depth thermocouple measurements, which holds also for actively cooled environments such as transpiration cooled surfaces using porous materials. A heat flux determination from in-depth thermocouples is of particular interest in high-temperature and chemically reactive environments such as combustion or fusion chambers and thermal protection systems. However, the classical analytical approaches are very difficult to apply in those environments. The main problems are the unknown mounting of the thermocouple and the cooling gas mass flow that leads to an increased internal heat transfer. In the paper the noninteger system identification method is applied to a transpiration cooled system. A thermocouple mounted in the porous structure measures temperature rise due to laser-induced radiative surface heat flux. The identification procedure shows that knowing cooling gas mass flow through the porous structure is sufficient to determine heat flux from the temperature data with an accuracy <16%. It is shown that the heat transfer at the surface does not disturb the method. This approach is useful for many applications of actively cooled structures, for example turbine blade measurements, combustion chamber diagnostic, or even fusion chamber wall measurements, where very high heat fluxes can only be withstood by actively cooled structures. An outlook is given that shows that this approach can be used also to determine the internal heat transfer.

I. Introduction

ACTIVE cooling mechanisms are used in many applications for thermal protection of surfaces in combustion chambers, rocket nozzles, gas turbine blades, and only recently structures of reentry vehicles [1–4]. The basic principle is to inject a cooling fluid close to the wall to reduce the wall heat load. In literature, the three different effects, i.e., film, transpiration, or effusion cooling, are named to occur in actively cooled structures. These cooling mechanisms, however, complicate the problem of the determination of a heat transfer coefficient to the wall and thus a calculation of the heat flux to the wall becomes challenging. Although transpiration cooling has been proven theoretically as an effective cooling mechanism by many investigators, its technological application became recently of particular interest with the invention of high-temperature porous material [2]. The progress in material development allows a very new approach to high-temperature environments. From rocket engine combustion chambers and nozzles to turbine blades, from thermal protection systems for reentry vehicles to fusion chamber walls, in all these modern high-temperature environments, transpiration cooling is currently in the focus of research to overcome the principle problem of exceeding the wall temperature limit [4–8].

Regenerative cooling is state of the art in rocket engines. Liquid fuel is used to cool the nozzle and the heated fuel is injected in the combustion chamber at higher temperature, which again increases the combustion efficiency. Results of numerical analysis show that the efficiency of regenerative cooling compared with transpiration cooling can lower the wall temperature by more than 30%. Transpiration cooling means that the fuel is injected through the wall into the combustion chamber or nozzle. This is advantageous because a layer of relatively cool fuel close to the wall protects the wall [5]. With the invention of high-temperature porous media for rocket engines, those numerically proved improvements could be verified by experimental tests [3].

For high-speed aircraft, material and cooling issues for both airframe and engine are the key elements which force the designer to limit the flight Mach number [9].

All these engineering problems face the fact that the heat flux at the surface is a design critical value yet difficult to measure. In the high heat flux regimes, a direct measurement is not applicable, since no sensor is available to measure directly at the surface. The only solution is therefore, a temperature measurement using in-depth temperature sensors. However, an inverse method has to be applied to determine surface heat flux. In the case of a transpiration cooling environment, however, the often applied one-dimensional analytical calculation is prone to error: The thermocouple position is of particular importance in this approach and particularly in a porous material very difficult to know with sufficient precision. Moreover, the porosity has to be known, which complicates this analytical problem further because there is not only the dependency from heat capacity, heat conductivity (both values needed for the porous material), but also from the material specific parameter of porosity. A numerical approach lacks a precise information of porosity of the material which is impossible to know for a particular sensor system. Finally, for such complex materials, the thermophysical properties are not known and difficult to determine. A recent publication of Shi and Wang presents a solution for this inverse problem [10]. Here, the accuracy of the method again depends strongly on the accuracy of the information about the specific heat capacity, heat conductivity, and coolant temperature.

In this paper, an approach based on the calibration of the real environment will be presented. For the analysis of the calibration measurement, the noninteger system identification (NISI) approach is applied to a transpiration cooled environment. Using basic calibration experiments, the transpiration cooling is inherently covered by the NISI calibration process. It is shown for the first time that the knowledge of the coolant mass flow is sufficient to determine the surface heat flux.

II. Theory

The basic approach of the NISI method is solving the inverse heat conduction problem by a noninteger system identification approach.

Presented as Paper 2010-4803 at the 27th AIAA Aerodynamic Measurement Technology and Ground Testing Conference, Chicago, IL, 28 June–1 July 2010; received 21 September 2010; revision received 29 December 2010; accepted for publication 30 January 2011.

*Researcher, Institut für Raumfahrtsysteme; loehle@irs.uni-stuttgart.de.
†Institut für Raumfahrtsysteme.

This method has first been published by Battaglia et al. [11]. System identification in general is the empirical mathematical description of the dependency of one physical quantity to one or more other quantities by means of characteristic measurements. In the present case, the measured temperature signal $T(t, x = b)$ at the measurement location b in the material is related to the net heat flux $q(t, x = 0)$ at the surface using fractional derivative expansions of the temperature and the heat flux data together with a priori unknown coefficients. These coefficients are identified in a calibration step. Heat flux is then determined from the inverse analysis of the temperature data. The NISI approach so far assumes linear behavior. For the present investigation, namely to proof the principal applicability of this method to cooled surfaces, the high-temperature effect was neglected. Thus, the linearity is given. The experimental setup was chosen to cover the time scales of interest (about 30 s) for the different applications.

Considering a one-dimensional heat equation and constant thermophysical properties, the heat equation becomes

$$\frac{\partial T}{\partial t}(x,t) = \frac{\lambda}{\rho c_p}\frac{\partial^2 T}{\partial x^2}(x,t) \qquad (x,t) \geq 0 \tag{1}$$

where ρ, c_p, and λ are the density, the heat capacity, and the heat conductivity of the material, respectively; T is the temperature and x is the coordinate of the dimension. The partial differential Eq. (1) can be solved via Laplace transformation. The transformation leads to the ordinary differential equation

$$\frac{\mathrm{d}^2\bar{T}(x,s)}{\mathrm{d}x^2} - \frac{s}{a}\bar{T}(x,s) = 0 \tag{2}$$

where s is the Laplace variable and here, $a = \lambda/(\rho c_p)$ is the thermal diffusivity. The solution using an exponential approach leads to

$$\bar{T}(x,s) = K_1(s)e^{-x\sqrt{s/a}} + K_2(s)e^{x\sqrt{s/a}} \tag{3}$$

The constants K_1 and K_2 are defined by the boundary conditions of the problem. In case of the one-dimensional semi-infinite heat conduction problem, the parameter $K_2 = 0$ and the solution of the problem in the Laplace domain is

$$H(x,s) = \frac{\bar{T}(x,s)}{\bar{\phi}(s)} = \frac{1}{\sqrt{s}\sqrt{\lambda\rho c_p}}e^{-x\sqrt{s/a}} \tag{4}$$

The heat flux signal $\phi(s)$ is transferred by the function $H(s)$ to a temperature signal. For problems with higher complexity, i.e., without the assumption of one-dimensional semi-infinite heat conduction, this transfer function can be written as the expansion

$$H(x,s) = \frac{\bar{T}(x,s)}{\bar{\phi}(s)} = \frac{1}{\sqrt{s}\sqrt{\lambda\rho c_p}}\sum_{n=0}^{\infty}\frac{(-1)s^{\frac{n-1}{2}}x^n}{(\frac{\lambda}{\rho c_p})^n n!} \tag{5}$$

The order of the exponent of s in the Laplace domain is the order of the differentiation in the time domain. According to the extension of this model function by Battaglia et al. [11], the general transfer function in the Laplace domain is of the form

$$H(s) = \frac{\sum_{n=L_0}^{L\to\infty}\beta_n s^{n/2}}{\sum_{n=M_0}^{M\to\infty}\alpha_n s^{n/2}} \tag{6}$$

which translates to

$$\sum_{n=M_0}^{M}\alpha_n D^{n/2}T(t) = \sum_{n=L_0}^{L}\beta_n D^{n/2}\phi(t) \quad \text{with} \quad \alpha_{M_0} = 1 \tag{7}$$

in the time domain. Battaglia et al. [11] showed that this model holds for many analytically known problems and only recently, Löhle et. al. [12,13] applied this method successfully to null-point calorimetry. As can be seen from Eq. (7), the system is characterized for $x \geq 0$ by the model parameters α_n and β_n and the noninteger differentiations $D^{n/2}$. It turns out that for most problems, a small number of parameters is sufficient. In the case of the semi-infinite half space, the amount of parameters is about five [13]. The advantage of this theoretical approach is that in Eq. (7), the thermophysical properties are inherently integrated. For one particular application, the knowledge of the parameters fully characterizes the sensor system and allows a determination of the surface heat flux from a temperature measurement inside the material. So far the only crucial assumption is that this is a linear function. Thus, the thermophysical properties have to be constant or the model parameters have to be determined at the distinct experimental condition, e.g., at higher temperatures. However, particularly for the use of composite materials, this approach offers some advantages: the knowledge of thermophysical properties are not required and thus also a possible anisotropy of these values are not of interest. Secondly, this identification method does not depend on the spatial diffusion of heat in the solid, thus one-dimensional or three-dimensional heat diffusion does not result in a higher complexity of the NISI procedure.

From the experimental standpoint, the system identification procedure means the determination of the unknown coefficients α_n and β_n using an appropriate measurement setup. Using these few calibration measurements, the system shall be calibrated for any other case. A system is completely characterized by its impulse response [14]. However, even a short laser radiation heat pulse does not cover the requirement of an impulse in the sense of the Dirac definition [13]. Therefore, a calibration measurement is performed where pulses of different lengths, usually defined in a pseudorandom series, are applied, which cover the range of pulses expected for the experimental condition to be investigated. In other words, each pulse duration corresponds to a certain frequency of the investigated system. With a theoretical Dirac impulse, all frequencies would be covered. Hence, the calibration using different frequencies that cover at least the range of measurement frequencies successfully characterizes the system, i.e., the objective is to have the power spectral density of the theoretical Dirac. The impulse response can then be calculated afterward from the calibrated system.

The implementation of the NISI approach in a usable computer code is described in detail by Battaglia et al. [11] and Gardarein et al. [15]. In general it is a least-square method to rebuild the temperature signal according to the known heat flux to identify the model parameters. The noninteger derivatives are calculated using an algorithm by Podlubny [16].

III. Experimental Setup

The experimental principle is to perform a calibration measurement using laser radiation to determine the unknown model parameters α_n and β_n. The absorption and emission characteristics of the system to be identified have to be known beforehand since the measurement is related to the net heat flux. In principle, a system is fully characterized by its impulse or step response, where the step response is the derivation of the impulse response [14]. Both a step and a Dirac impulse are not feasible to be experimentally realized.

Figure 1 shows the experimental setup. The calibration step within the present study is performed using a diode laser system as the

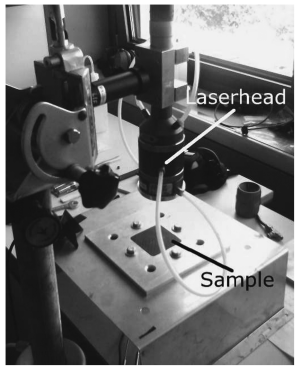

Fig. 1 Experimental setup for calibration.

radiation heat flux source. The laser system is a commercial system from Laserline GmbH of type LDF. It consists of stapled laser diode assemblies that are driven by a front panel. The power level and timing can be programmed with a simple programming language integrated in the laser system software. The laser output is fed via a fiber optic cable to the laser head, where collimating optics are attached. Additionally, a focusing lens system can be added. In the present case it has only been used to vary the laser spot dimension. Finally, only the collimating lens system has been used to cover the biggest possible area on the porous sample. The laser output covers then an area of 42 mm in diameter. Figure 1 shows the laser head as mounted in front of the actively cooled structure. The laser spot energy profile could not be measured within this study. It is assumed that, due to the fiber optical setup, the laser profile is a flat top profile. The laser energy has been measured separately using a calorimetric sensor provided by DLR, German Aerospace Center. The real laser heating has been observed using a fast photo diode (Thorlabs DET200) and after testing the measured photo diode voltage signals have been related to the measured calorimetric energy values. The emissivity of the material has been taken into account ($\epsilon = 0.85$) to get the net heat flux into the structure. This approach has also been tested during the calorimetric energy measurements for consistency.

The actively cooled structure is squared and has an edge length of 50 mm. It is pressed in a metallic support where from the backside the cooling gas is fed into a reservoir below the ceramic structure. From this reservoir it is assumed that the gas is homogeneously pressed through the porous material (see Fig. 2). Depending on the porous channels through the material, the gas flowing out of the surface passed a more or less long path within the material. From optical inspection it is assumed that the outflow is very homogeneous. However, this is not of particular importance for the application of the present method, since a possible discontinuity in the coolant gas flow at the surface due to material inhomogeneities is taken into account by the calibration step.

The thermocouple is a shielded 1 mm type *K* thermocouple which is fed through the reservoir. It is glued into a hole in the ceramic structure using a two-component ceramic adhesive. Because of experimental constraints for the cooling gas flow, a mounting of the thermocouples parallel to the isotherms was not feasible. Although this leads to less accuracy in the temperature measurement, the effect itself is included in the NISI calibration method. Data acquisition has been realized using a AD210 high-performance isolation amplifier and a LeCroy Wavesurfer 24Xs oscilloscope for analogue digital conversion. All data, i.e., temperature and diode, are stored on the same time base using the oscilloscope. All cables are shielded and the shielding is grounded on the same potential as the oscilloscope. The material has been characterized for porosity, heat conductivity, and heat capacity. However, these data were not available nor required for the present investigation. From pure visible inspection, the fibers seem to be arranged in-plane, which therefore should be the direction of higher heat conductivity. The porosity of these materials, defined as the volume percentage of air with respect to the overall volume, is usually rather low, i.e., <30% [17]. Consequently, it can be assumed that the heat conduction is primarily driven by the solid structure. The results show that this assumption is reasonable from the point of view of the NISI approach.

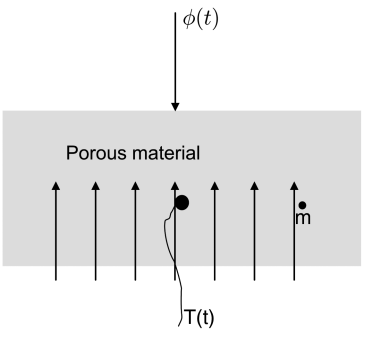

Fig. 2 Sketch of the setup.

IV. Results

Figure 3 shows two exemplary data sets. As can be seen, each heat flux pulse is very constant. A fluctuation of about 5 kW/m^2 can be seen. This, however, is due to the data acquisition noise of the oscilloscope. The laser system itself is not able to generate such fast fluctuations in a 5 kW/m^2 range. This holds for all performed measurements. The measured temperature is significantly lowered due to the active cooling. In between the pulses is a low heat flux, which is due to the diode laser power system. The high power supply is in a standby modus where a small amount of diode laser power ($\approx$20 kW/m^2) is already emitted. This modus guarantees short rise times for the actual heat pulses.

The sample rate of the measurement data is 500 Hz. As mentioned, the identification of the transfer function is conducted by least-square fitting to the acquired temperature profile. Since the relative change in temperature induced by a surface heat flux is independent of the absolute temperature value, a baseline for the analysis of the signal has to be defined. Thus, preprocessing of the measurement data is required before the existing algorithm can be applied. The temperature signal is leveled so as the value at the start of the measurement is 0. Consequently, the present signal-to-noise ratio of the data decreases from about 42 dB to 21 dB. To dampen the now relevant influence of noise on the identification process, a low pass filter is applied. The chosen filter is a running window Gaussian frequency filter. The cutoff frequency is set at 1 Hz, assuming that changes are larger than 1 Hz. Following the filter application, a measurement data reduction down to 25 Hz is performed.

To keep the computational costs acceptable, the amount of thermophysical parameters that characterize the system has to be finite. In the present case, the amount of parameters is limited to 13, resulting in a transfer function of the form

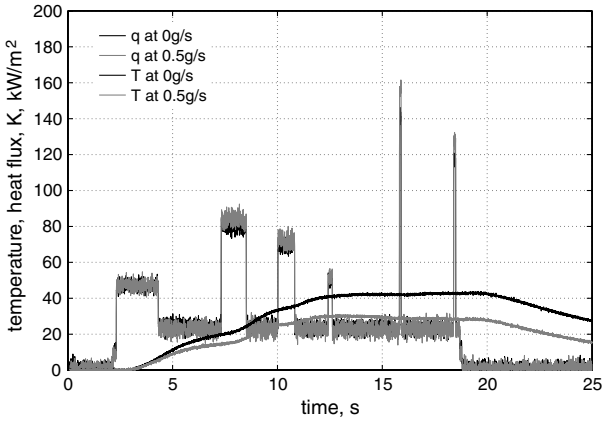

Fig. 3 Calibration data (temperature and calibration heat flux) without flow and with 0.5 g/s gas mass flow.

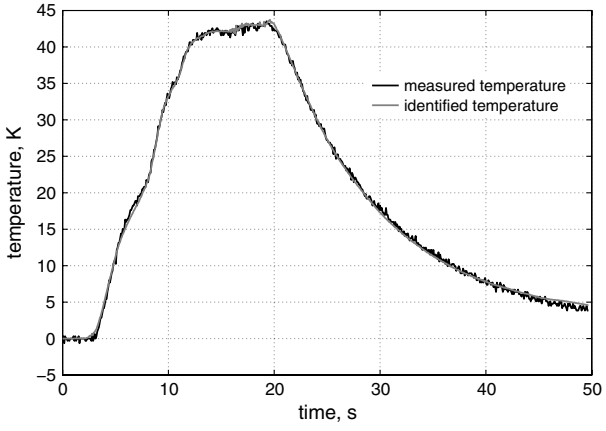

Fig. 4 Temperature curve and least-square fitted data for identification.

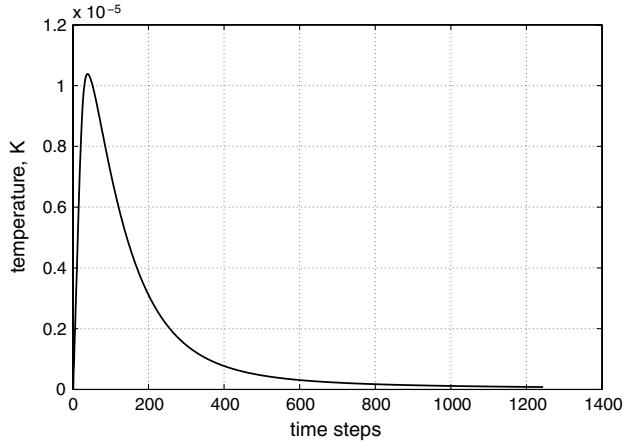

Fig. 5 Impulse response as calculated from identified system for 0 g/s.

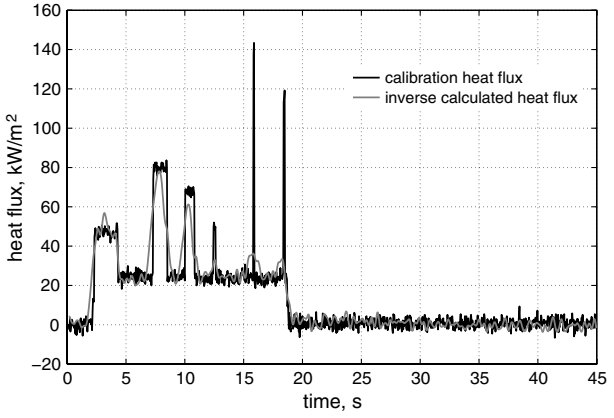

Fig. 6 Calibration heat flux and identified heat flux using the NISI approach.

$$H(s) = \frac{\sum_{n=0}^{n=9} \beta_n s^{n/s}}{\sum_{n=0}^{n=2} \alpha_n s^{n/s}} \tag{8}$$

Within the time frame of the measurement, these limitations provide reasonable determination of the system behavior. Figure 4 shows exemplary the result of the calibration without active cooling compared with the measured temperature progression. The calculated impulse response, characterizing the system for 0 g/s cooling gas mass flow, is shown in Fig. 5. An inversion can be performed using the identified system, i.e., the impulse response (see Fig. 5) and the measured temperature profile are used which should result in the calibration heat flux profile. Figure 6 shows this for the case presented in Fig. 4. The identified parameters of the transfer function for $\alpha_0 = 1$ are presented in Table 1. The accuracy of the fit is always better than 0.7 for the α_i and $10^{-}5$ for the β_i. As can be seen, the very short peaks of only 80 ms length are not rebuilt. However, this is not astonishing since the system does not react on these very short pulses as can be seen from Fig. 2. Here, the short pulse does not result in a significant temperature rise at the measurement location. This is due to the heat conduction behavior of the material. The heat diffuses, according to the thermophysical properties, faster in the direction of the higher heat conductivity. Assuming an orthotropic behavior heat conduction in fiber direction is faster. Thus, the thermocouple below the surface is not affected by this short time heat flux.

The presented steps for the 0 g/s have been performed in the same manner for different gas mass flow conditions. Although not presented, the least-square fits are as good as the one presented. The calculated impulse responses for the different gas mass flows are shown in Fig. 6. With higher cooling gas mass flows, the amplitude of the impulse response is consequently reduced. Thus, the surface heat flux is reduced with increasing cooling gas mass flow. Since radiation heat flux is used this effect can not be based on a surface heat flux change by influencing the calibration heat flux, e.g., by higher convection due to higher gas mass flow. The method uses the net heat flux and convection is obviously not of importance [18]. However, to investigate this effect, numerical simulations with different surface heat transfer coefficients h have been conducted. This simulation is intended to investigate whether the higher blowing ratio results theoretically in higher convection close to the surface due to this higher gas mass flow through the wall which would then affect the calibration. Boundary conditions are chosen to match semi-infinite, one-dimensional behavior. The NISI method has been applied to this computer model and the impulse response is identified for different heat transfer coefficient settings at the surface of the computer model. Figure 7 shows the result. As can be seen, in a reasonable domain of heat transfer coefficients, which is $0 < h < 100$ W/(m^2 K), the impulse response is not affected. This means that there is no effect of surface convection. Thus, the cooling of the present investigation is based on internal convection of the cooling gas mass flow.

The starting time of the rise of the impulse response is a direct measure for the penetration time, i.e., the time it takes until a thermocouple at a distance x from the surface in the material reacts on a surface heat flux. Analytically, the penetration time for semi-infinite media is

$$t_p = \left(\frac{x}{3,6 \sqrt{\frac{\lambda}{\rho c_p}}} \right)^2 \tag{9}$$

For typical room temperature values of the thermophysical properties for carbon fiber ceramics, the penetration time is of the order of milliseconds [19]. In Fig. 8, a change in penetration time is not seen for the different cooling gas mass flows. This shows, that the main heat conduction path is heat conduction in the solid. Thus, the time it takes to reach the thermocouple is for all cases the same. The gas cooling then means that it transports more heat with increasing gas flow while the heat conduction from the surface to the sensor remains unchanged. The behavior is similar to studies where the sensor remains at the same position, but the material's heat capacity increases.

Table 1 Parameters of the transfer function for varying cooling gas mass flows

$\dot{m}$	0.000 g/s	0.108 g/s	0.201 g/s	0.298 g/s	0.609 g/s	0.702 g/s
α_1	0.5651	0.7179	0.7012	0.2355	−0.0895	−0.3348
α_2	4.0706	3.7428	3.3747	3.5834	3.2909	3.3245
β_0	2.20e − 3	2.10e − 3	2.00e − 3	1.60e − 3	1.20e − 3	1.06e − 4
β_1	−4.10e − 3	−4.00e − 3	−3.80e − 3	−3.00e − 3	−2.10e − 3	−2.69e − 4
β_2	3.50e − 3	3.40e − 3	3.30e − 3	2.50e − 3	1.70e − 3	2.99e − 4
β_3	−1.70e − 3	−1.70e − 3	−1.70e − 3	−1.20e − 3	−7.61e − 4	−1.90e − 4
β_4	5.68e − 4	5.72e − 4	5.77e − 4	3.87e − 4	2.19e − 4	7.65e − 5
β_5	−1.24e − 4	−1.26e − 4	−1.31e − 4	−8.15e − 5	−4.12e − 5	−2.01e − 5
β_6	1.83e − 5	1.87e − 5	1.98e − 5	1.15e − 5	5.02e − 6	3.48e − 6
β_7	−1.73e − 6	−1.78e − 6	−1.94e − 6	−1.03e − 6	−3.77e − 7	−3.80e − 7
β_8	9.61e − 8	9.89e − 8	1.11e − 7	5.45e − 8	1.54e − 8	2.40e − 8
β_9	−2.38e − 9	−2.45e − 9	−2.83e − 9	−1.27e − 9	−2.45e − 10	−6.65e − 10

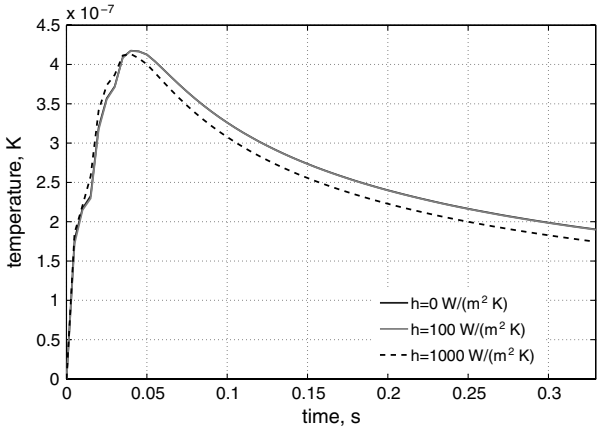

Fig. 7 Impulse responses for increasing heat transfer coefficient h at the surface.

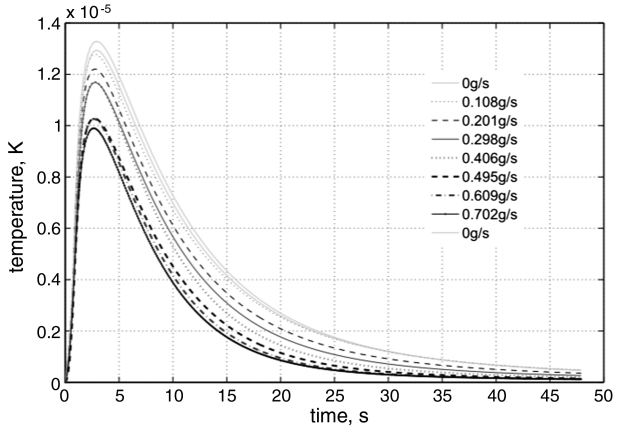

Fig. 8 Impulse responses for different coolant gas mass flows.

V. Conclusions

The paper presents the very first results of the application of the NISI method to transpiration cooled ceramic material to determine the surface heat flux from in-depth thermocouple measurement. In contrast to analytical and numerical methods, the advantage of the NISI method is that neither the thermophysical properties nor the exact position of the thermocouple have to be known, since a calibration measurement is performed that takes these values into account. Within the present investigation, this method has been extended to actively cooled structures, exemplary using a porous ceramic material with gaseous cooling gas mass flow. The NISI method treats the heat conduction problem as a control oriented system. A heat flux at the boundary surface leads to a temperature rise of a sensor inside the material. It has been shown within this paper that the impulse response fully characterizes the sensor system also for a problem including porous materials. The impulse response is significantly influenced by a varying cooling gas mass flow. The amplitude reduces when the cooling gas mass flow is increased. Numerical simulations show that surface convection does not affect the method and is not of relevance for this problem. Because the impulse response is not delayed with increasing cooling gas mass flow, it is shown that the penetration time is not affected by the cooling and, therefore, the main heat conduction occurs in the solid while the cooling leads to a heat transport to the outer surface, similar to solid materials with increasing heat capacity. As an outlook, this method could be applied to determine the thermophysical properties of these materials. If a well-defined geometry were set up with defined boundary conditions, the internal heat transfer could be determined from the calibration measurements.

Acknowledgment

The authors greatfully thank DLR, German Aerospace Center for providing the material as well as the laser system to perform these tests.

References

[1] Glass, D. E., Dilley, A. D., and Kelly, H. N., "Numerical Analysis of Convection/Transpiration Cooling," *Journal of Spacecraft and Rockets*, Vol. 38, No. 1, 2001, pp. 15–20. doi:10.2514/2.3666

[2] v. Wolfersdorf, J., "Effect of Coolant Side Heat Transfer on Transpiration Cooling," *Heat and Mass Transfer*, Vol. 41, No. 4, 2004, pp. 327–337. doi:10.1007/s00231-004-0549-x

[3] Greuel, D., Herbertz, A., Haidn, O., Ortelt, M., and Hald, H., "Transpiration Cooling Applied to C/C Liners of Cryogenic Liquid Rocket Engines," *40th Joint Propulsion Conference*, AIAA 2004-3682, 2004.

[4] Böhrk, H., Kuhn, M., and Weihs, H., "Concept of the Transpiration Cooling Experiment on SHEFEX II," *2nd International ARADays*, EUCASS, Moscow, 2008.

[5] Landis, J., and Bowman, W. J., "Numerical Study of a Transpiration Cooled Rocket Nozzle," *34th Joint Propulsion Conference*, AIAA 1996-2580, 1996.

[6] Heufer, K. A., and Olivier, H., "Film Cooling for Hypersonic Flow Conditions," *14th Hypersonic Conference*, AIAA 2006-8067, 2006.

[7] Bussard, R. W., "Fusion as Electric Propulsion," *Journal of Propulsion and Power*, Vol. 6, No. 5, 1990, pp. 567–574. doi:10.2514/3.23257

[8] Youchison, D. L., Lutz, T. J., Williams, D., and Nygren, R. E., "High Heat Flux Testing of a Helium Cooled Tungsten Tube with Porous Foam," *Fusion Engineering and Design*, Vol. 82, Nos. 15–24, 2007, pp. 1854–1860. doi:10.1016/j.fusengdes.2007.04.004

[9] Soller, S., Kirchberger, C., Kuhn, M., Langener, T., Bouchez, M., and Steelant, J., "Experimental Investigation of Cooling Techniques and Materials for Highspeed Flight Propulsion Systems," *16th AIAA Hypersonics Conference*, AIAA 2009-7374, 2009.

[10] Shi, J., and Wang, J., "Inverse Problem of Estimating Space and Time Dependent Hot Surface Heat Flux in Transient Transpiration Cooling Process," *International Journal of Thermal Sciences*, Vol. 48, No. 7, 2009, pp. 1398–1404. doi:10.1016/j.ijthermalsci.2008.11.019

[11] Battaglia, J.-L., Cois, O., Puigsegur, L., and Oustaloup, A., "Solving an Inverse Heat Conduction Problem Using a Non-Integer Identified Model," *International Journal of Heat and Mass Transfer*, Vol. 44, No. 14, 2001, pp. 2671–2680. doi:10.1016/S0017-9310(00)00310-0

[12] Löhle, S., Battaglia, J.-L., Batsale, J.-C., Enouf, O., Dubard, J., and Filtz, R.-R., "Characterization of a Heat Flux Sensor Using Short Pulse Laser Calibration," *Review of Scientific Instruments*, Vol. 78, No. 5, 2007, pp. 053501–053506. doi:10.1063/1.2736388

[13] Löhle, S., Battaglia, J.-L., Jullien, P., van Ootegem, B., Couzi, J., and Lasserre, J.-P., "Improvement of High Heat Flux Measurements Using a Null-Point Calorimeter," *Journal of Spacecraft and Rockets*, Vol. 45, No. 1, 2008, pp. 76–81. doi:10.2514/1.30092

[14] Ljung, L., *System Identification: Theory for the User*, Prentice–Hall, Upper Saddle River, NJ, 1987.

[15] Gardarein, J.-L., Battaglia, J.-L., and Löhle, S., "Heat Flux Sensor Calibration Using Noninteger System Identification: Theory, Experiment, and Error Analysis," *Review of Scientific Instruments*, Vol. 80, No. 2, 2009, pp. 025103–025108. doi:10.1063/1.3079328

[16] Podlubny, I., *Fractional Differential Equations*, Academic Press, New York, 1998.

[17] Gülhan, A., Ed., *RESPACE: Key Technologies for Reusable Space Systems*, Notes on Numerical Fluid Mechanics, Springer, New York, 2008.

[18] Marineau, E. C., and Rennie, R. M., "Investigation of the Importance of Convective Heating Transfer on Laser-Induced Heating," *Journal of Thermophysics and Heat Transfer*, Vol. 24, No. 3, 2010, pp. 573–580. doi:10.2514/1.47657

[19] Kaviany, M., *Principles of Heat Transfer*, Wiley, New York, 2001.